Heliyon 10 (2024) e32115

Contents lists available at ScienceDirect

Heliyon

journal homepage: www.cell.com/heliyon

Research article

A multi-omics method for breast cancer diagnosis based on metabolites in exhaled breath, ultrasound imaging, and basic clinical information

Yuan Yang [a], Huiling Long [d], Yong Feng [b], Shuangming Tian [a], Haibin Chen [b,c,**], Ping Zhou [a,*]

[a] Department of Ultrasound, The Third Xiangya Hospital, Central South University, Changsha, 410013, China
[b] Breax Laboratory, PCAB Research Center of Breath and Metabolism, Beijing, 100071, China
[c] Digital Medicine Division, Guangzhou Sinohealth Digital Technology Co., Ltd., Guangzhou, 510000, China
[d] Hunan Drug Evaluation and Adverse Reaction Monitoring Center

ARTICLE INFO

Keywords:
Breast cancer
Volatile organic compounds
Breath
High-pressure photon ionization time-of-flight mass spectrometry
Automated breast volume scanner
Radiomics

ABSTRACT

Background and aims: Through a nested cohort study, we evaluated the diagnostic performance of breath-omics in differentiating between benign and malignant breast lesions, and assessed the diagnostic performance of a multi-omics approach that combines breath-omics, ultrasound radiomics, and clinic-omics in distinguishing between benign and malignant breast lesions.
Materials and methods: We recruited 1,723 consecutive patients who underwent an automated breast volume scanner (ABVS) examination. Breath samples were collected and analyzed by high-pressure photon ionization time-of-flight mass spectrometry (HPPI-TOF-MS) to obtain breath-omics features. 238 of 1,723 enrolled participants have received pathological confirmation of breast nodules finally. The breast lesions of the 238 participants were contoured manually based on ABVS images for ultrasound radiomics feature calculation. Then, single- and multi-omics models were constructed and evaluated for breast nodules diagnosis via five-fold cross-validation.
Results: The area under the curve (AUC) of the breath-omics model was 0.855. In comparison, the multi-omics model demonstrated superior diagnostic performance for breast cancer, with sensitivity, specificity, and AUC of 84.1 %, 89.9 %, and 0.946, respectively. The multi-omics performance was comparable to that of the Breast Imaging Reporting and Data System (BI-RADS) classification via senior ultrasound physician evaluation.
Conclusion: The multi-omics approach combining metabolites in exhaled breath, ultrasound imaging, and basic clinical information exhibits superior diagnostic performance and promises to be a non-invasive and reliable tool for breast cancer diagnosis.

1. Introduction

Breast cancer is the most prevalent tumor globally, with an estimated 2.261 million new cases and 685,000 deaths globally in 2020 [1]. In China, breast cancer is the most common malignancy among women, and ranks fifth in cause of cancer-induced mortalities. The

* Corresponding author.
** Corresponding author. Digital Medicine Division, Guangzhou Sinohealth Digital Technology Co., Ltd., Guangzhou, 510000, China.
E-mail addresses: haibinc@hotmail.com (H. Chen), Zhouping1000@hotmail.com (P. Zhou).

https://doi.org/10.1016/j.heliyon.2024.e32115
Received 24 August 2023; Received in revised form 27 May 2024; Accepted 28 May 2024
Available online 28 May 2024

Abbreviation

ABVS	Automated breast volume scanner
AUC	Area under the curve
BI-RADS	Breast Imaging Reporting and Data System
VOCs	Volatile organic compounds
ROI	Region of interest
HPPI-TOF-MS	High-pressure photon ionization time-of-flight mass spectrometry

incidence of breast cancer is continuously increasing [1].

Imaging screening can detect breast cancer at an early stage, allowing for early interventions, which are crucial to improving the prognosis of breast cancer patients. Asian women often have dense breast tissue and, according to the recommendations of the American College of Radiology, breast ultrasound should be used to screen these patients [2]. However, breast ultrasound screening relies on ultrasound physicians who visually observe and describe the sonographic features of the lesion, followed by lesion categorization using the Breast Imaging Reporting and Data System (BI-RADS) [3]. This process is time-consuming and subjective, depending on the ultrasound physician's interpretation, leading to inevitable errors in diagnosis. Traditional breast ultrasound screening also has false negative and positive rates as high as 33.3 % and 20.2 %, respectively [4]. Therefore, the development of more objective and accurate diagnostic tools is of great significance for the early diagnosis of breast cancer patients.

Radiomics, as an emerging field, offers a promising approach to this development. By converting imaging into high-dimensional data, radiomics can extract microscale lesion features that are not visible to the naked eye, providing a comprehensive reflection of the lesion's information [5]. The selection of potentially meaningful features can be objectively quantified or used to build machine learning models, which could provide an almost instantaneous diagnosis of lesions without the need for manual intervention [6–8]. In Li J's study, the deep learning-based models built on ultrasound images have good diagnostic performance in differentiating between benign and malignant breast lesions (AUC = 0.94) [9], predicting molecular subtypes of breast cancer (AUC = 0.87) [10] and axillary lymph node metastasis in breast cancer patients (AUC = 0.95) [11]. The automated breast volume scanner (ABVS) is an emerging ultrasound technology that automatically scans the breast to obtain ultrasound images, overcoming the operator dependency associated with handheld ultrasound [12,13]. Therefore, ultrasound radiomics based on ABVS offers higher automation and reproducibility. Furthermore, multi-omics studies, including metabolomics, can provide additional information on breast cancer characteristics from different perspectives [14]. By combining ultrasound radiomics with other omics features, it may be possible to develop diagnostic tools with higher diagnostic performance.

Human exhalation contains hundreds of trace volatile organic compounds (VOCs) [15], leading to the development of a new branch of breath-omics in metabolomics. Machine learning models based on breath-omics have value in the diagnosis of breast cancer [16–19], and some VOC features related to breast cancer have been discovered [20]. There are various methods to determine VOCs in exhaled air, each with its advantages and disadvantages (Supplementary Table 1). Gas chromatography-mass spectrometry (GC-MS) requires complex preprocessing of the collected gas and involves cumbersome procedures [21]. Although electronic nose technology is portable and easy to use, its detection limits are insufficient for quantitative or qualitative analysis of VOCs [22]. High-pressure photoionization time-of-flight mass spectrometry (HPPI-TOF-MS) enables qualitative and quantitative analysis of VOCs in exhaled air under high humidity and ambient temperature conditions, without any gas preprocessing. HPPI-TOF-MS also has high sensitivity, capable of detecting VOCs in exhaled air at concentrations as low as 10 parts per trillion (ppt) [23], making it a very promising detection technique.

A standardized workflow has been established using HPPI-TOF-MS for the collection, detection, and data processing of exhaled VOCs, and has validated the feasibility of this technology in detecting diseases such as breast cancer [24], lung cancer [25], esophageal cancer [26], tuberculosis [27], and Covid-19 [28]. We aimed to integrate breath-omics, ultrasound radiomics, and clinical features to construct a multi-omics machine learning model, to develop a more accurate, objective, and automated non-invasive diagnostic tool for breast cancer.

2. Materials and methods

2.1. Patients

This nested cohort study recruited consecutive patients who underwent ABVS examination at The Third Xiangya Hospital of Central South University in China from March 2022 to December 2022. Patients were screened according to the inclusion and exclusion criteria, and the study obtained approval from our institutional ethics committee. The inclusion criteria were as follows: 1) age 18–75 years; 2) planned ABVS examination; 3) signed written informed consent to participate in the study. We excluded patients as per the following criteria: 1) pre-existing conditions that hindered the exhalation of sufficient breath samples; 2) underwent general anesthesia within the past 10 days before breath collection; 3) has a previous history of malignant tumors; 4) received anti-tumor treatments such as radiation therapy, chemotherapy, or targeted therapy; 5) currently breastfeeding; 6) pregnant or planning to become pregnant. As illustrated in Fig. 1a and ,723 participants were pre-enrolled in this study, and 13 refused participation, all other patients signed written informed consent. Breath samples were then collected from all participants at the same location, while the air around the

sampling site was sampled, and ultrasound images and clinical information were subsequently collected. Those with invalid breath samples, poor ABVS image quality, and incomplete clinical information were excluded. Of the remaining participants, 238 underwent surgery or aspiration biopsy. Based on the pathology results, 77 were finally identified with breast cancer, with 82 malignant and 168 benign breast lesions confirmed by pathological results.

2.2. ABVS examination

ABVS examinations were performed using the Siemens ACUSON S2000 ultrasound scanner with a high-frequency linear array transducer (model 14L5BV) operating at frequencies ranging from 5.0 to 12.0 MHz, maximum scanning volume of 154 mm × 168 mm × 60 mm. Patients were positioned supine with their arms raised above their heads to fully expose the breasts, and the scanner was applied with appropriate pressure. A replaceable membrane was placed on the scanner surface to ensure sufficient contact with the skin. The instrument settings were preconfigured based on the size of the patient's breasts. Scans were performed in the median, lateral, medial, or other non-standardized orientations of both breasts. After the scan, the position of the nipple was marked, and the acquired transverse and sagittal plane images were uploaded to the image processing workstation for image reconstruction, including the generation of coronal and 3D images. An experienced senior ultrasound physician with 20 years of expertise in breast ultrasound examination blindly reviewed the ABVS images without knowledge of clinical pathology information. The physician assessed the acoustic image characteristics of the lesions and determined the BI-RADS classification (class 3/4a/4b/4c/5). According to the study by Elverici et al. malignant characteristics of the lesions included spiculated margin, irregular shape, nonparallel orientation, peripheral hyperechoic halo, posterior acoustic pattern attenuation, and microcalcifications. Additionally, one malignant characteristic was classified as class 4a, two as class 4b, three as class 4c, and more than three as class 5 [29].

2.3. Basic clinical information

Basic clinical information of possible clinical significance was collected, including gender, age, body mass index (BMI), history of alcohol use, smoking and cancer, family history of cancer, drug use, and comorbidities. BMI was calculated based on the patient's self-reported height and weight, while the remaining information was obtained from the patient's medical records.

2.4. Image segmentation and feature extraction

A junior ultrasound physician with 3 years of experience in breast ultrasound examination, who was unaware of the pathological information, used the annotation tool "ITK-SNAP" (www.itksnap.org) to manually delineate the entire tumor region of interest (ROI) along the edge of the lesion on axial, sagittal, and coronal ABVS images. The ROI included the breast lesion but not the area surrounding the lesion (Fig. 2a–c). In cases where the lesion boundaries were indeterminate, a consensus decision was made in discussion with an experienced senior ultrasound physician. Lesions were labeled with different values for patients with multiple nodules. Before feature extraction, the images were preprocessed using the morphological operation to obtain the clean lesion region with the surrounding region set as zero. Feature extraction was performed for the lesion region using the Pyradiomics package, version 3.0 (https://pyradiomics.readthedocs.io/en/latest/changes.html#pyradiomics-3-0) [30], and the extracted features included First Order Statistics (18 features), Shape-based (3D) (14 features), Gray-Level Co-occurrence Matrix (24 features), Gray-Level Run-Length Matrix (16 features), Gray-Level Size Zone Matrix (16 features), Neighbouring Gray Tone Difference Matrix (5 features), and Gray-Level

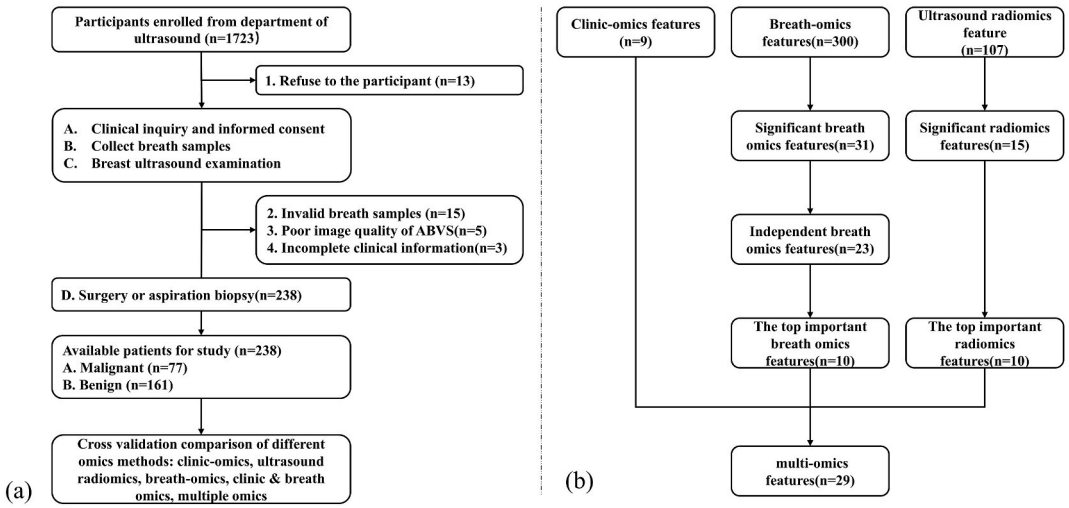

Fig. 1. Flowcharts of **(a)** participant recruitment and **(b)** multi-omics feature selection.

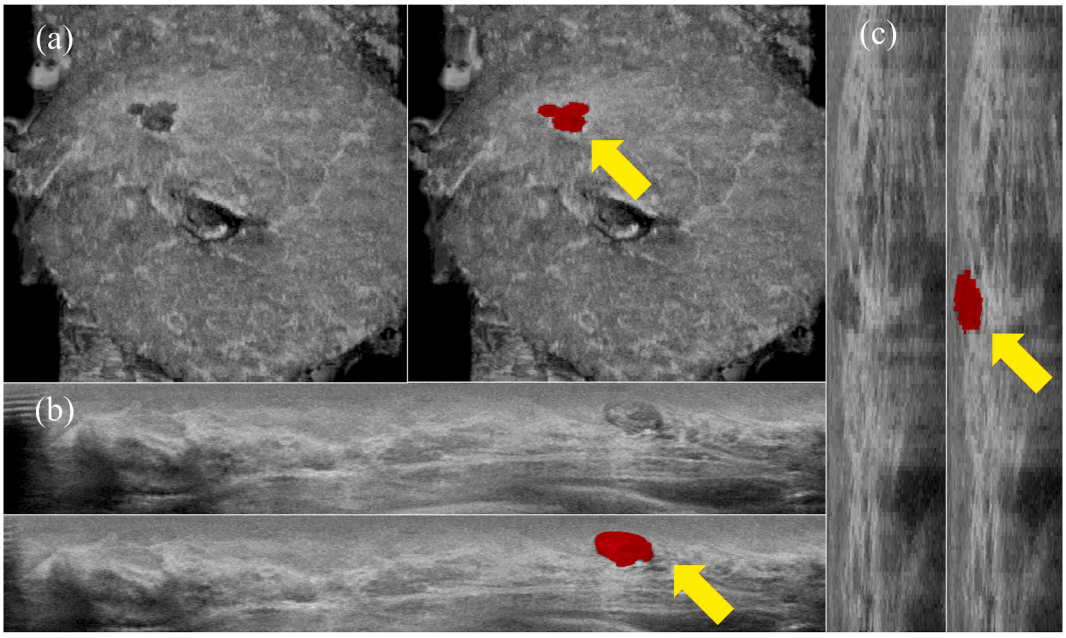

Fig. 2. Diagram of the region of interest (ROI) outline of breast lesions. **(a)** Invasive ductal carcinoma ABVS coronal plane images; **(b)** fibroadenoma ABVS transversal plane images; **(c)** intraductal papilloma ABVS sagittal plane images.

Dependence Matrix (14 features).

2.5. Breath sample collection and analysis

We set standard sampling demands and protocols to minimize the possible effects of daily diet, smoking, alcohol, and environment on exhaled gas VOC. Firstly, the participants were required to prepare for sampling in advance under the following conditions: no smoking, alcohol, or food within an hour before sampling. Secondly, participants were required to clean their mouths with purified water just before sampling. Thirdly, all samples were collected at the same site to minimize the effect of any environmental factors. Lastly, deep inhalation and exhalation training were executed for each participant, to homogenize the collection of gases contained in a complete deep breath. With a deep nasal inhalation, participants completely exhaled the breath into a 1.2-L volume sampling bag made of polyether-ether-ketone (PEEK) via a disposable gas nipple. At the same time as the exhaled gas sampling, we collected the ambient gas. A novel online high-pressure photon ionization time-of-flight mass spectrometry (HPPI-TOF-MS) was used for breath sample detection and analysis, as employed and evaluated for breath sample detection in multiple studies [24–26]. In simple terms, after the gas is introduced into the sample introduction system, gas-phase ions are generated through high-pressure photon ionization (HPPI). These gas-phase ions are then separated based on their mass-to-charge ratio using a time-of-flight mass analyzer (TOF). Subsequently, an ion transmission system transfers the separated gas-phase ions to a microchannel plate (MCP) detector to measure the content of volatile organic compounds (VOCS) in each sample. This system does not require any preprocessing before gas analysis. For more details about HPPI-TOF-MS, please refer to our previous article [23]. In HPPI-TOF-MS, soft ionization is achieved by a commercial VUV-Kr lamp with a photon energy of 10.6 eV to predominantly produce radical cations ($M+$) which are formed as $M + h\gamma \rightarrow M+ + e$, which can ionize most VOCs in the breath gas. With the HPPI-TOF-MS detection, the VOCs with m/z in the range of [20, 320] were detected. In this study, the area of the strongest peak in the range of [x-0.5, x+0.5] was calculated and regarded as the feature of VOC with m/z of x. Thus, 300 breath-omics features were extracted via breath detection for further study. In HPPI-TOF-MS. The standard sample with nitrogen as the carrier gas, with a mixed combination of nine compounds (Acetone, furan, Benzene, Aniline, Styrene, n-propylbenzene, Cinene, Perchloroethylene, Hexachloro-1,3-butadiene) at 1 ppm concentration was used for the equipment calibration before daily testing for quality control.

2.6. Model development

To select valuable multiple omics features and avoid model over-fitting, different feature selection strategies were executed for different omics features. As shown in Fig. 1b, all clinic-omics features with possible significance were included directly. The breath-omics features with no significant differences ($p > 0.05$) between malignant and benign groups were excluded first. Then, the VOC ions with low intensity but highly correlated with other selected VOC ions (correlation coefficient >0.9) among all samples were excluded. Finally, a random forest (RF) model was constructed on the whole data set, and the ten most important VOC ions were selected based on the feature importance or coefficient. For the ultrasound radiomics features, a similar feature selection procedure was also executed

as that for breath-omics with the correlation analysis-based feature selection was removed. Therefore, 29 multi-omics features(10 breath-omics, 10 ultrasound raidomics, and 9 clinic-omics) were used for the breast cancer diagnosis mode construction. In this study, the ensemble method of three classical machine learning methods including RF, logistic regression, and eXtreme Gradient Boosting (XGB) was employed as the classifier for breast cancer diagnosis model construction based on single- and multi-omics. Considering that the data set was small, five-fold cross-validation was adopted for more adequate model evaluation. Specifically, the data set was evenly divided into five parts, one of which was taken as the validation set, and the rest as the training set each time, until all data was validated.

2.7. Statistical analysis

To evaluate the diagnostic performance of the multi-omics model to differentiate between benign and malignant breast lesions, the model results were compared with the pathological diagnosis results. We calculated the sensitivity, specificity, accuracy, AUC, and the relative 95 % confidence interval (CI). All statistical analyses were performed using SAS version 9.4 (SAS Institute Inc., Cary, NC, USA) and Origin software (version 2018). Descriptive statistics were reported as frequencies (percentages) for categorical variables or median (interquartile range [IQR]) for continuous variables. We compared the basic clinical features among different patient groups using the Mann–Whitney *U* test and Chi-square test. A p-value <0.05 was considered statistically significant for all the analyses. The DeLong test was used for the ROC comparison among single- and multi-omics models. All the tests were two-tailed.

3. Results

3.1. Basic clinical features

The basic clinical features of all patients are illustrated in Table 1. A total of 238 cases were finally included for the single- and multi-omic method evaluation in the study, with 161 cases being classified as benign and 77 as malignant. The age, BMI, family history of cancer, history of cancer, comorbidities, and drug use were significantly different between participants with malignant and benign nodules (p-value <0.05). There was no bias in gender, history of alcohol use, or smoking. Based on the pathological results of 250 breast nodules, 168 nodules were benign, and 82 nodules were malignant, as shown in Table 2.

3.2. Breast cancer diagnosis performance

Fig. 3 shows the classification performance of the breast cancer diagnosis model in each fold of cross-validation. The ultrasound radiomics model achieved the worst performance, with AUC <0.8 in each cross-validation fold (Fig. 3b). In comparison, the clinic-omics and breath-omics models achieved better performances, with AUCs >0.8 in three and four cross-validation folds, respectively (Fig. 3a and c). By combining the clinic- and breath-omics, the performance of the model was further improved, with AUC >0.85 in each cross-validation fold (Fig. 3d). Furthermore, the multi-omics involving ultrasound radiomics features achieved better performance than the double-omics model (clinic & breath), with AUC >0.90 in each cross-validation fold (Fig. 3e). As illustrated in Fig. 3, the models were robust on different cross-validation folds.

As illustrated in Table 3 and Fig. 4, the overall performance and qualitative metrics also show the diagnostic power ranking as multi-omics > double-omics > breath-omics > clinic-omics > ultrasound radiomics. The overall AUC of the multi-omics model was

Table 1
The basic clinical features of 238 patients.

		All (n = 238)	Malignant (n = 77)	Benign (n = 161)	p-values
Age	Median (IQR)	42 (33, 51)	51 (45, 55)	37 (30, 46)	**<0.001**[a]
Gender (%)	Male	1 (0.4 %)	0 (0 %)	1 (0.6 %)	1.000[b]
	Female	237 (99.6 %)	77 (100 %)	160 (99.4 %)	
BMI	Median (IQR)	21.4 (20.2, 23.2)	22.6 (20.3, 25.1)	21.1 (20.0, 22.6)	**0.001**[a]
Smoke (%)	Smoker	1 (0.4 %)	0 (0 %)	1 (0.6 %)	0.705[b]
	Non-smoker	237 (99.6 %)	77 (100 %)	160 (99.4 %)	
Alcohol (%)	Drinker	1 (0.4 %)	1 (1.3 %)	0 (0 %)	1.000[b]
	Non-drinker	237 (99.6 %)	76 (98.7 %)	161 (100 %)	
Family history of cancer (%)	Presence	8 (3.4 %)	6 (7.8 %)	2 (1.2 %)	**0.025**[b]
	Absence	230 (96.6 %)	71 (92.2 %)	159 (98.8 %)	
History of cancer (%)	Presence	8 (3.4 %)	6 (7.8 %)	2 (1.2 %)	**0.025**[b]
	Absence	230 (96.6 %)	71 (92.2 %)	159 (98.8 %)	
Comorbidity* (%)	Presence	36 (15.1 %)	26 (33.8 %)	10 (6.2 %)	**<0.001**[b]
	Absence	202 (84.9 %)	51 (66.2 %)	151 (93.8 %)	
Drug use* (%)	Presence	11 (4.6 %)	11 (14.3 %)	0 (0.0 %)	**<0.001**[b]
	Absence	227 (95.3 %)	66 (85.7 %)	161 (100 %)	

Notes: P-value <0.05 was considered statistically significant. [a]: Mann-Whitney *U* test. [b]: Chi-square test. IQR: Interquartile Range. *Comorbidity includes pulmonary nodules, fatty liver, hepatic cyst, cardiovascular disease, hypertension, diabetes, renal cyst, and kidney stones. Drugs include antihypertensive or diabetes drugs.

Table 2
Pathology of 250 breast lesions.

Benign Lesion	Number (168)	Malignant Lesion	Number (82)
Fibroadenoma	110	Invasive ductal carcinoma	65
Adenosis	29	Ductal carcinoma in situ	12
Papilloma	17	Mucinous carcinoma	2
Cyst	5	Metaplastic carcinoma	2
Granulomatous inflammation	4	Invasive lobular carcinoma	1
Sclerosing adenosis	2	/	/
Suppurative inflammation	1	/	/

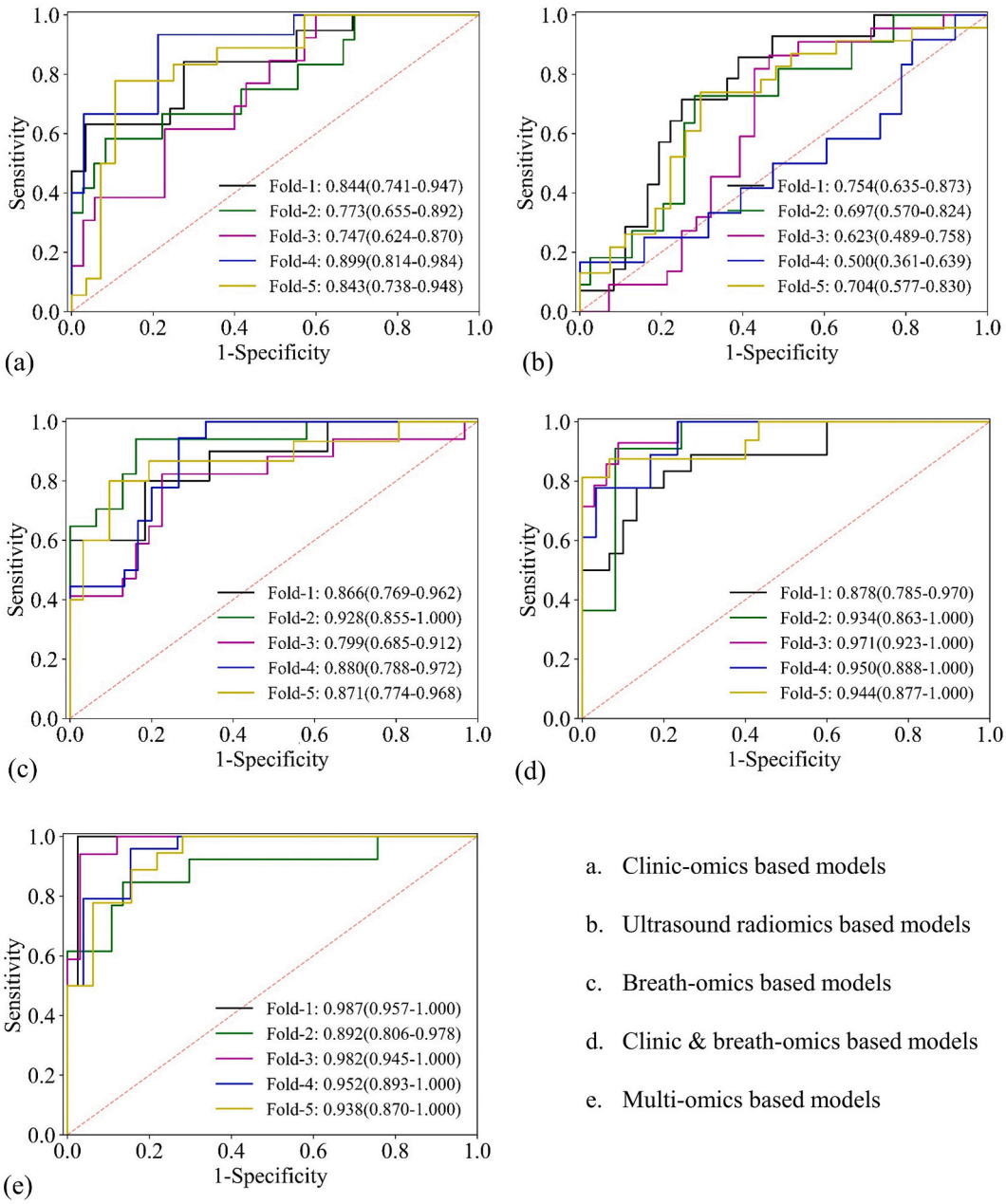

Fig. 3. The ROC curves of clinic-omics **(a)**, radiomics **(b)**, breath-omics **(c)**, clinic & breath-omics **(d)**, and multi-omics **(e)** methods in each fold of the five-fold cross-validation. ROC, receiver operating characteristic.

0.938 (95 % CI, 0.908–0.968). By setting the cut-off value as 0.5, the multi-omics model could achieve a sensitivity, specificity, and accuracy of 84.1 % (95 % CI, 75.1–93.2 %), 89.9 % (95 % CI: 85.3–94.4 %), and 88.0 % (95 % CI: 84.0–92.0 %), respectively (Table 3). In comparison, a higher AUC of 0.973 (95 % CI, 0.953–0.994) was achieved via manual BI-RADS scores. Based on clinical decision principles, BI-RADS 4b and above lesions are generally considered malignant. However, if we set the malignant threshold at BI-RADS 4a, the corresponding sensitivity, specificity, and accuracy of the BI-RADS scores were 98.7 % (95 % CI, 96.2–100 %), 70.2 % (95 % CI: 63.1–77.3 %), and 79.4 % (95 % CI: 74.3–84.5 %), respectively. If the malignant threshold was set as BI-RADS 4b, the sensitivity, specificity, and accuracy were 87.0 % (95 % CI, 79.0–95.1 %), 99.4 % (95 % CI: 98.2–100 %), and 95.4 % (95 % CI: 92.7–98.0 %), respectively. Moreover, we employed the DeLong test to analyze the significance of the differences in AUC curves. As illustrated in Table 4, there are significant differences between any two omics methods, except for breath-omics vs clinic-omics, and multi-omics vs clinic& breath omics. There is no significant difference between BI-RADS, clinic & breath omics, and multi-omics.

3.3. Potential VOC markers

There were 31 VOC ions with significant differences between the malignant and benign groups. Considering that part VOCs would produce protonated ions, we excluded those with low intensity but highly correlated with other selected VOC ions. Finally, we analyzed the top 10 VOC ions involved in breast cancer diagnosis. As illustrated in Fig. 5, compared to the benign participants, nine VOCs (m/z = 105, 119, 116, 45, 104, 77, 58, 90, 133) showed significantly depressed concentration in participants with malignant lesions, and one VOC with m/z of 138 showed significantly elevated concentration.

Since the qualitative ability of the HPPI-TOF-MS is limited, we can infer the possible chemicals of these key VOC ions based on their m/z (105, 119, 116, 45, 104, 138, 77, 58, 90, 133), correlation, intensity distribution, other published potential biomarkers, and the human breath-omics database. As illustrated in Table 5, these VOCs would be potential biomarkers of breast cancer. The chemical of VOC ions with m/z of 104 and 105 would be pentanethiol; 119, 116, and 138, 2-butoxyethanol, isobutyl acetate, and creosol, respectively; 45, the fragment of carboxylic acids or esters; 77, 1-propanethiol or methylthioethane; and 58, 90, and 133, acetone, diethyl sulfide, and 2-methylbenzoxazole, respectively. Due to inconsistencies in sample collection and analysis and participant status, the 10 key VOCs identified above are heterogeneous with those found in previous studies to be associated with breast cancer [31]. We made a preliminary comparison with previous studies according to the category to which the organics found belonged, as shown in Supplementary Fig. 1.

Similarly, we analyzed the top 10 ultrasound radiomics features between the malignant and benign groups. As illustrated in Table 6, five Shape, 2 Gy-Level Run-Length Matrix (GLRLM), 2 Gy-Level Dependence Matrix (GLDM), and 1 Gy-Level Size Zone Matrix (GLSZM) based features were finally selected to determine the malignant and benign breast nodules. These shape-based features represent the basic geometric parameters of breast nodules. These GLRLM, GLDM, and GLSZM based features represent the texture information of breast nodules, mainly related to the inhomogeneous breast nodules. These key ultrasound radiomics features are consistent with the ultrasound physician's view of the breast lesions.

4. Discussion

In this study, we validated our machine learning model for exhaled gas VOC detection based on HPPI-TOF-MS has potential diagnostic capability in differentiating benign and malignant breast lesions. By integrating clinical features, the diagnosis performance was further enhanced, proposing a new, convenient, rapid, and accurate method to diagnose breast cancer. Furthermore, the multi-omics model combining breath-omics, ultrasound radiomics, and clinic-omics demonstrated superior diagnostic performance compared to single-omics models.

We employed the HPPI-TOF-MS technique for the online analysis of exhaled VOCS, presenting significant advantages in non-invasiveness, ease of operation, and high sensitivity, as evidenced by the high acceptance rate among patients (99.2 %) and the strong classification efficacy of the breath-omics model (AUC = 0.855) in our study. When compared to ultrasound radiomics(68.4 %) or clinic-omics(78.2 %), breath-omics(80.3 %) had higher accuracy. It implies exhaled VOCs, being the final manifestation of body metabolism, can better express whether the subject has breast cancer. After integrating multiple omics information, the diagnostic performance of the model was further enhanced, this signifies the value of multi-dimensionally integrating patient information to improve the accuracy of breast cancer diagnosis as previous studies, The specific VOCs found in this study were different to those reported in previous studies [16,20,24,32], although the categories of these VOCs were similar. This may be attributed to various factors, including differences in sample sizes, study methods, population heterogeneity, sample processing, and statistical analysis

Table 3
Quantitative evaluation metrics and the corresponding 95 % confidence intervals of the BC diagnosis model in five-fold cross-validation.

Method	Cut-off	Sensitivity (%)	Specificity (%)	Accuracy (%)	AUC
Clinic-omics	0.5	67.5 (55.3, 79.8)	83.2 (77.5, 89.0)	78.2 (72.9, 83.4)	0.832 (0.785, 0.880)
Ultrasound radiomics		46.3 (32.2, 60.4)	79.2 (73.0, 85.3)	68.4 (62.6, 74.2)	0.673 (0.614, 0.731)
Breath-omics		62.3 (49.0, 75.6)	88.8 (84.0, 93.7)	80.3 (75.2, 85.3)	0.855 (0.810, 0.899)
Clinic & Breath-omics		76.6 (65.7, 87.5)	93.2 (89.3, 97.1)	87.8 (83.7, 92.0)	0.929 (0.896, 0.962)
Multi-omics		84.1 (75.1, 93.2)	89.9 (85.3, 94.4)	88.0 (84.0, 92.0)	0.946 (0.918, 0.974)
BI-RADS	4a	98.7 (96.2, 100)	70.2 (63.1, 77.3)	79.4 (74.3, 84.5)	0.973 (0.953, 0.994)
BI-RADS	4b	87.0 (79.0, 95.1)	99.4 (98.2, 100)	95.4(92.7, 98.0)	

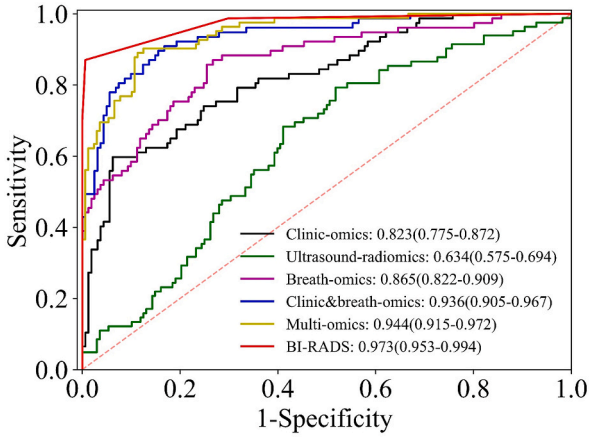

Fig. 4. The overall ROC curves of the clinic-omics, ultrasound radiomics, breath-omics, clinic & breath-omics, and multi-omics methods in the five-fold cross-validation and the BI-RADS classification on ultrasound image by senior ultrasound physician. ROC, receiver operating characteristic.

Table 4
ROC curve comparison results of different combined omics approaches using the DeLong test.

DeLong test	radiomics	Clinic-omics	Breath-omics	Clinic & breath omics	Multi-omics	BI-RADS
Radiomics	1.000	<0.001	<0.001	<0.001	<0.001	<0.001
Clinic-omics	<0.001	1.000	0.310	<0.001	<0.001	<0.001
Breath-omics	<0.001	0.310	1.000	0.001	0.004	<0.001
Clinic & breath omics	<0.001	<0.001	0.001	1.000	0.624	0.073
Multi-omics	<0.001	<0.001	0.004	0.624	1.000	0.109
BI-RADS	<0.001	<0.001	<0.001	0.073	0.109	1.000

Notes: The values in the table represent p-values obtained from the DeLong test, used to compare the statistical significance differences among various omics approaches in ROC curve analysis.

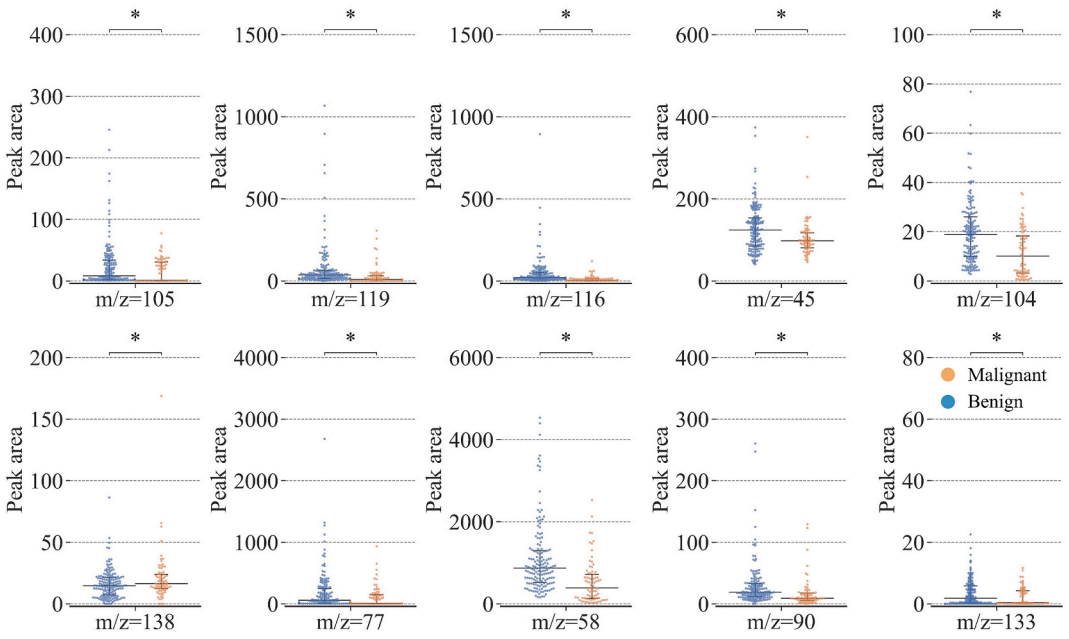

Fig. 5. Comparison of the 10 most important VOC ions for differentiating between malignant and benign groups.

Table 5
The key VOCs associated with BC diagnosis.

m/z	Potential VOCs	CAS number	Molecular weight	Molecular formula
105	Pentanethiol	110-66-7	104.214	$C_5H_{12}S(+H)$
119	2-Butoxyethanol	111-76-2	118.174	$C_6H_{14}O_2(+H)$
116	Isobutyl acetate	110-19-0	116.158	$C_6H_{12}O_2$
45	Fragment of carboxylic acids or esters	/	~45	$COOH^+$
104	Pentanethiol	110-66-7	104.214	$C_5H_{12}S$
138	Creosol	93-51-6	138.164	$C_8H_{10}O_2$
77	1-Propanethiol/methylthioethane	107-03-9/624-89-5	76.161	$C_3H_8S(+H)$
58	Acetone	67-64-1	58.079	C_3H_6O
90	Diethyl sulfide	352-93-2	90.187	$C_4H_{10}S$
133	2-Methylbenzoxazole	95-21-6	133.147	C_8H_7NO

Notes: VOCs: Volatile Organic Compounds. CAS: Chemical Abstracts Service Number, CAS number is a unique numerical identifier used to distinguish chemical substances.

Table 6
The key ultrasound radiomics features associated with BC diagnosis.

Radiomics groups	Descriptions	Malignant	Benign	P-value
GLRLM	Run-length non-uniformity	6652.4 ± 7364.4	3521.2 ± 6952.5	0.002
GLRLM	Gray-level non-uniformity	23327.6 ± 24799.5	14021.2 ± 22901.0	0.004
GLDM	Dependence entropy	3.8 ± 1.1	3.4 ± 1.1	0.016
Shape	Surface area	55305.4 ± 60098.8	33307.3 ± 50570.7	0.003
Shape	Maximum 3D diameter	185.4 ± 87.0	140.5 ± 90.4	<0.001
Shape	Maximum 2D diameter row	175.9 ± 84.0	128.9 ± 82.8	<0.001
Shape	Minor axis length	78.3 ± 36.9	62.4 ± 43.1	0.005
GLDM	Dependence variance	35.1 ± 8.3	32.4 ± 8.6	0.021
GLSZM	Size zone non-uniformity	92.6 ± 133.4	51.4 ± 126.0	0.019
Shape	Maximum 2D diameter slice	177.9 ± 84.7	135.0 ± 86.8	<0.001

Notes: All p-values were calculated using independent samples t-tests. GLRLM: Gray-Level Run-Length Matrix. GLDM: Gray-Level Dependence Matrix. GLSZM: Gray-Level Size Zone Matrix.

approaches, as well as variations in environmental and specific conditions. Future studies should further explore the impact of breast cancer subtypes, disease stages, sample sources, and environmental factors on VOC profiles to better understand the metabolic characteristics of breast cancer and improve diagnostic accuracy [17,33]. Taking these factors into account, our study provides new insights into the field of VOC analysis in breast cancer and offers directions and inspirations for further research.

In terms of ultrasound radiomics characterization,We found that the values of texture features (GLRLM, GLSZM, GLDM) were significantly increased in breast cancer. This finding is consistent with previous research [34,35], indicating that the internal composition of malignant tumors are typically more complex and heterogeneous than benign tumors. Additionally, the values of morphological features in breast cancer were also significantly higher compared to benign breast lesions [29], which implies that breast cancers have larger dimensions, more irregular shapes, and internal structures compared to benign breast nodules. Therefore, these radiomic features may serve as useful tools for the diagnosis of breast cancer.

The diagnostic performance of the ABVS-based BI-RADS classification in this study was similar to the results of previous studies [36,37], particularly with a sensitivity of up to 98.7 % when using BI-RADS 4a as the benign-malignant cut-off value. However, a flaw is still apparent, heavily dependent on the ultrasound physician performing the BI-RADS classification, hence the performance fluctuation. Although the multi-omics model has a slightly lower sensitivity than the BI-RADS classification, its specificity is better, it also has the advantage of objectivity, easy access to information and a high degree of automation, making it a complementary technology to BI-RADS.

Our study also has some limitations. Firstly, there are significant biases in several clinic characteristics, although they are risk factors of breast cancer. Future prospective studies still need to be designed to control confounding factors. Secondly, this study was conducted in a single center and had a limited number of included cases. Further external validation with a larger sample size and multiple-center studies is needed to evaluate the reliability of the breath-omics and multi-omics models. Thirdly, all radiomics features of breast lesions were extracted from stored images, which may result in information omission or misjudgment, leading to suboptimal performance of the individual ultrasound radiomics model. At last, only one junior ultrasound physician (with 3 years of experience in breast ultrasound) manually delineated the ROIs used to extract the radiomics features, which may introduce intra- or inter-observer biases. In future studies, we will incorporate a step of senior physician review of the ROI or use semi-automatic or fully automatic segmentation methods based on deep learning networks to further improve the diagnostic performance and automation level of the model.

5. Conclusions

Our findings indicate that breath-omics has significant potential value in breast cancer diagnosis and should receive more attention. The diagnostic performance of multi-omics machine learning model is superior to that of single-omics models and comparable to the diagnostic ability of experienced ultrasound physicians. This indicates that integrating breath-omics, ultrasound radiomics, and clinic-omics can provide a more comprehensive reflection of the characteristics of breast cancer patients. Therefore, the multi-omics approach is a promising tool for automated and reliable diagnosis of breast cancer. However, further validation studies are needed before clinical application can be realized.

Ethics statement

The study was conducted in accordance with the Declaration of Helsinki, and approved by the Ethics Committee of the Third Xiangya Hospital (快 I 22099, approval date: 24 May 2022).

Funding

The work was supported by the National Natural Science Foundation of China [grant No. 81871367].

Data availability statement

The datasets supporting the findings of this study are available in the Mendeley Data repository at https://doi.org/10.17632/h7fvhycmmn.1, and these data can be accessed openly.

CRediT authorship contribution statement

Yuan Yang: Writing – review & editing, Writing – original draft, Visualization, Validation, Software, Project administration, Methodology, Investigation, Formal analysis, Data curation, Conceptualization. **Huiling Long:** Methodology. **Yong Feng:** Software. **Shuangming Tian:** Methodology. **Haibin Chen:** Writing – review & editing, Validation, Supervision, Resources, Conceptualization. **Ping Zhou:** Writing – review & editing, Validation, Supervision, Resources, Funding acquisition, Conceptualization.

Declaration of competing interest

The authors declare that they have no known competing financial interests or personal relationships that could have appeared to influence the work reported in this paper.

Acknowledgment

Thanks to all members of the Department of Ultrasound, Third Xiangya Hospital, Central South University for their help in the manuscript preparation.

Appendix A. Supplementary data

Supplementary data to this article can be found online at https://doi.org/10.1016/j.heliyon.2024.e32115.

References

[1] H. Sung, J. Ferlay, R.L. Siegel, et al., Global cancer statistics 2020: GLOBOCAN Estimates of incidence and Mortality Worldwide for 36 cancers in 185 countries, CA Cancer J Clin 71 (3) (2021) 209–249.
[2] R.D. Rosenberg, D. Seidenwurm, Optimizing breast cancer screening programs: experience and structures, Radiology 292 (2) (2019) 297–298.
[3] D.A. Spak, J.S. Plaxco, L. Santiago, M.J. Dryden, B.E. Dogan, BI-RADS((R)) fifth edition: a summary of changes, Diagn Interv Imaging 98 (3) (2017) 179–190.
[4] W.A. Berg, Z. Zhang, D. Lehrer, et al., Detection of breast cancer with addition of annual screening ultrasound or a single screening MRI to mammography in women with elevated breast cancer risk, JAMA 307 (13) (2012) 1394–1404.
[5] F. Pesapane, P. De Marco, A. Rapino, et al., How radiomics can improve breast cancer diagnosis and treatment, J. Clin. Med. 12 (4) (2023).
[6] W.Q. Luo, Q.X. Huang, X.W. Huang, H.T. Hu, F.Q. Zeng, W. Wang, Predicting breast cancer in breast imaging reporting and data system (BI-RADS) ultrasound category 4 or 5 lesions: a nomogram combining radiomics and BI-RADS, Sci. Rep. 9 (1) (2019) 11921.
[7] P. Johannet, N. Coudray, D.M. Donnelly, et al., Using machine learning algorithms to predict immunotherapy response in patients with advanced melanoma, Clin. Cancer Res. 27 (1) (2021) 131–140.
[8] P. Courtiol, C. Maussion, M. Moarii, et al., Deep learning-based classification of mesothelioma improves prediction of patient outcome, Nat. Med. 25 (10) (2019) 1519–1525.
[9] J. Li, Y. Bu, S. Lu, et al., Development of a deep learning-based model for diagnosing breast nodules with ultrasound, J. Ultrasound Med. 40 (3) (2021) 513–520.
[10] M. Jiang, D. Zhang, S.C. Tang, et al., Deep learning with convolutional neural network in the assessment of breast cancer molecular subtypes based on US images: a multicenter retrospective study, Eur. Radiol. 31 (6) (2021) 3673–3682.

[11] Q. Sun, X. Lin, Y. Zhao, et al., Deep learning vs. Radiomics for predicting axillary lymph node metastasis of breast cancer using ultrasound images: don't forget the peritumoral region, Front. Oncol. 10 (2020) 53.
[12] M. Zanotel, I. Bednarova, V. Londero, et al., Automated breast ultrasound: basic principles and emerging clinical applications, Radiol. Med. 123 (1) (2018) 1–12.
[13] X. Lin, M. Jia, X. Zhou, et al., The diagnostic performance of automated versus handheld breast ultrasound and mammography in symptomatic outpatient women: a multicenter, cross-sectional study in China, Eur. Radiol. 31 (2) (2021) 947–957.
[14] G. Saini, K. Mittal, P. Rida, E.A.M. Janssen, K. Gogineni, R. Aneja, Panoptic view of prognostic models for personalized breast cancer management, Cancers 11 (9) (2019).
[15] B. de Lacy Costello, A. Amann, H. Al-Kateb, et al., A review of the volatiles from the healthy human body, J. Breath Res. 8 (1) (2014) 014001.
[16] J. Li, Y. Peng, Y. Liu, et al., Investigation of potential breath biomarkers for the early diagnosis of breast cancer using gas chromatography-mass spectrometry, Clin. Chim. Acta 436 (2014) 59–67.
[17] C. Wang, B. Sun, L. Guo, et al., Volatile organic metabolites identify patients with breast cancer, cyclomastopathy, and mammary gland fibroma, Sci. Rep. 4 (2014) 5383.
[18] G. Peng, M. Hakim, Y.Y. Broza, et al., Detection of lung, breast, colorectal, and prostate cancers from exhaled breath using a single array of nanosensors, Br. J. Cancer 103 (4) (2010) 542–551.
[19] M. Phillips, R.N. Cataneo, B.A. Ditkoff, et al., Prediction of breast cancer using volatile biomarkers in the breath, Breast Cancer Res. Treat. 99 (1) (2006) 19–21.
[20] G.B. Hanna, P.R. Boshier, S.R. Markar, A. Romano, Accuracy and methodologic challenges of volatile organic compound-based exhaled breath tests for cancer diagnosis: a systematic review and meta-analysis, JAMA Oncol. 5 (1) (2019) e182815.
[21] D.J. Beale, F.R. Pinu, K.A. Kouremenos, et al., Review of recent developments in GC-MS approaches to metabolomics-based research, Metabolomics 14 (11) (2018) 152.
[22] A.D. Wilson, Advances in electronic-nose technologies for the detection of volatile biomarker metabolites in the human breath, Metabolites 5 (1) (2015) 140–163.
[23] Y. Wang, J. Jiang, L. Hua, et al., High-pressure photon ionization source for TOFMS and its application for online breath analysis, Anal. Chem. 88 (18) (2016) 9047–9055.
[24] J. Liu, H. Chen, Y. Li, et al., A novel non-invasive exhaled breath biopsy for the diagnosis and screening of breast cancer, J. Hematol. Oncol. 16 (1) (2023) 63.
[25] S. Meng, Q. Li, Z. Zhou, et al., Assessment of an exhaled breath test using high-pressure photon ionization time-of-flight mass spectrometry to detect lung cancer, JAMA Netw. Open 4 (3) (2021) e213486.
[26] Q. Huang, S. Wang, Q. Li, et al., Assessment of breathomics testing using high-pressure photon ionization time-of-flight mass spectrometry to detect esophageal cancer, JAMA Netw. Open 4 (10) (2021) e2127042.
[27] L. Fu, Y. Feng, T. Ren, et al., Detecting latent tuberculosis infection with a breath test using mass spectrometer: a pilot cross-sectional study, Biosci Trends 17 (1) (2023) 73–77.
[28] P. Zhang, T. Ren, H. Chen, et al., A feasibility study of Covid-19 detection using breath analysis by high-pressure photon ionization time-of-flight mass spectrometry, J. Breath Res. 16 (4) (2022).
[29] E. Elverici, A.N. Barca, H. Aktas, et al., Nonpalpable BI-RADS 4 breast lesions: sonographic findings and pathology correlation, Diagn Interv Radiol 21 (3) (2015) 189–194.
[30] J.J.M. van Griethuysen, A. Fedorov, C. Parmar, et al., Computational radiomics system to decode the radiographic phenotype, Cancer Res. 77 (21) (2017) e104–e107.
[31] V. Vassilenko, P.C. Moura, M. Raposo, Diagnosis of carcinogenic pathologies through breath biomarkers: present and future trends, Biomedicines 11 (11) (2023).
[32] M. Mangler, C. Freitag, M. Lanowska, O. Staeck, A. Schneider, D. Speiser, Volatile organic compounds (VOCs) in exhaled breath of patients with breast cancer in a clinical setting, Ginekol. Pol. 83 (10) (2012) 730–736.
[33] O. Barash, W. Zhang, J.M. Halpern, et al., Differentiation between genetic mutations of breast cancer by breath volatolomics, Oncotarget 6 (42) (2015) 44864–44876.
[34] R.D. Chitalia, D. Kontos, Role of texture analysis in breast MRI as a cancer biomarker: a review, J. Magn. Reson. Imag. 49 (4) (2019) 927–938.
[35] W. Chen, M.L. Giger, H. Li, U. Bick, G.M. Newstead, Volumetric texture analysis of breast lesions on contrast-enhanced magnetic resonance images, Magn. Reson. Med. 58 (3) (2007) 562–571.
[36] X. Lin, J. Wang, F. Han, J. Fu, A. Li, Analysis of eighty-one cases with breast lesions using automated breast volume scanner and comparison with handheld ultrasound, Eur. J. Radiol. 81 (5) (2012) 873–878.
[37] H.Y. Wang, Y.X. Jiang, Q.L. Zhu, et al., Differentiation of benign and malignant breast lesions: a comparison between automatically generated breast volume scans and handheld ultrasound examinations, Eur. J. Radiol. 81 (11) (2012) 3190–3200.